Received 7 May 2019; revised 8 July 2019; accepted 13 August 2019. Date of publication 22 August 2019; date of current version 30 September 2019.
The review of this article was arranged by Editor K. Shenai.

Digital Object Identifier 10.1109/JEDS.2019.2937008

Stable Operation of AlGaN/GaN HEMTs for 25 h at 400°C in air

SALEH KARGARRAZI [1], (Member, IEEE), ANANTH SARAN YALAMARTHY [2], (Member, IEEE), PETER F. SATTERTHWAITE [3], SCOTT WILLIAM BLANKENBERG [4], CAITLIN CHAPIN [1], AND DEBBIE G. SENESKY [1], (Member, IEEE)

1 Department of Aeronautics and Astronautics, Stanford University, Stanford, CA 94305, USA
2 Department of Mechanical Engineering, Stanford University, Stanford, CA 94305, USA
3 Department of Electrical Engineering and Computer Science, Massachusetts Institute of Technology, Cambridge, MA 02142, USA
4 Department of Electrical Engineering, Stanford University, Stanford, CA 94305, USA

CORRESPONDING AUTHOR: S. KARGARRAZI (e-mail: skargar@stanford.edu)

This work was supported in part by the Knut and Alice Wallenberg Foundation, in part by the National Science Foundation Engineering Research Center for Power Optimization of Electro-Thermal Systems (POETS) under Award EEC-1449548, in part by the National Nanotechnology Coordinated Infrastructure (NNCI) under Award ECCS-1542152, and in part by the National Aeronautics and Space Administration under Award NNNX17AG44G and Award NNX17AG42G.

ABSTRACT Extreme environments such as the Venus atmosphere are among the emerging applications that demand electronics that can withstand high-temperature oxidizing conditions. While wide-bandgap technologies for integrated electronics have been developed so far, they either suffer from gate oxide and threshold voltage (V_{th}) degradation over temperature, large power supply requirements, or intrinsic base current. In this letter, AlGaN/GaN high electron mobility transistors (HEMTs) are suggested as an alternative platform for integrated sensors and analog circuits in extreme environments in oxidizing air atmosphere over a wide temperature range from 22°C to 400°C. An optimal biasing region, with a peak of transconductance ($g_{m,peak}$) at −2.3 V with a negligible shift over the temperature range was observed. Moreover, remarkably low V_{th} variation of 0.9% was observed, enabling the design of analog circuits that can operate over the entire temperature range. Finally, the operation of the devices at 400°C and 500°C over 25 hours was experimentally studied, demonstrating the stability of the DC characteristics after the 5 hours of burn-in, at 400°C.

INDEX TERMS Gallium nitride (GaN), high electron mobility transistor (HEMT), high-temperature electronics.

I. INTRODUCTION

Wide-bandgap semiconductors such as silicon carbide (SiC) and gallium nitride (GaN) have proven to be viable candidates for operation in extreme environments due to their superior electronic properties, namely low intrinsic carrier concentration [1], [2]. Wide-bandgap electronics have recently found use in aviation, space exploration, automotive and deep-well drilling applications. NASA Glenn Research center (GRC) has studied SiC JFETs (junction field effect transistors) for harsh environments for approximately a decade [3] and demonstrated reliable electronics operational at 500°C for one year [4]. High-temperature devices and circuits in SiC have also been studied in n-type metal-oxide semiconductor (NMOS) and complementary metal-oxide semiconductor (CMOS) [5]–[8], and BJT (bipolar junction transistor) [9]–[18]. The high-temperature SiC MOSFETs suffer from gate oxide and V_{th} degradation, while SiC JFETs demand large power supplies and SiC BJTs need a constant base current to operate. To address the need for low-power and high-temperature electronics, AlGaN/GaN high electron mobility transistor (HEMTs) are suggested.

AlGaN/GaN HEMTs are a promising candidate for implementation of integrated electronics [19]–[22], and a few studies have discussed the high-temperature capability of the HEMTs [23]–[25]. However, as compared with SiC, AlGaN/GaN HEMTs have not been sufficiently matured for implementation of integrated circuits (ICs) for extreme temperatures. Previous work has investigated the

This work is licensed under a Creative Commons Attribution 4.0 License. For more information, see http://creativecommons.org/licenses/by/4.0/

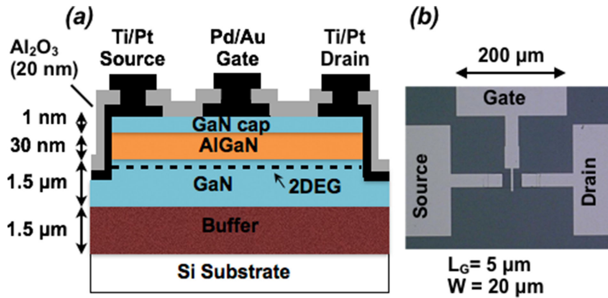

FIGURE 1. (a) The cross section schematic and (b) the micro-photograph of the AlGaN/GaN HEMT ($L_{GS} = L_{GD} = 6\ \mu$m).

high-temperature properties of AlGaN/GaN HEMTs, at temperatures of 200°C [26], 400°C [27], and 425°C [28]. Maier *et al.* [24] reported the failure of the GaN HEMTs with $Al_{0.24}Ga_{0.76}N$ barrier layer grown on SiC, with Ti/Al/Ni/Au Ohmic contacts and Mo/Au Schottky gate contact after 219 hours at 500°C in vacuum (benign environment). The corresponding failure was associated with the gate diode breakdown. In [29], among other tests, temperature step stress test has been conducted on AlGaN/GaN to study the reliability of the devices until failure. However due to the nature of the reliability test, limited discussions on the variation of the DC characteristics over temperature has been provided. Furthermore, the DC characteristics of AlGaN/GaN HEMTs and MIS-HEMTs have been studied up to 600°C in air for 30 minutes and the HEMTs fail prematurely at 300°C due to the high gate leakage [30]. The MIS-HEMTs operated up to 600°C, however, exhibit (V_{th}) instability beyond 300°C. Besides, formation of bubbles is observed above 300°C on the Ni/Au gates. In another study, the gate leakage in Pd/Au gates has shown to be lower than WSi, Ni, and Ir-based gates [31]. This is especially crucial at elevated temperatures, where the gate leakage tends to exacerbate.

In this letter, we investigate high-temperature operation of AlGaN/GaN HEMTs on Si substrates for analog ICs from 22°C up to 400°C. It is shown that the AlGaN/GaN HEMTs exposed to 400°C environments have a stable response over 25 hours of operation with $\sim$ 1% variation of V_{th} after 5-hours burn-in. Moreover, we show that the prolonged exposure to temperatures above 400°C in air can limit the operation of the AlGaN/GaN HEMTs due to the reduction of the 2DEG (2D electron gas) sheet density and mobility.

II. ALGAN/GAN HEMT FABRICATION

The HEMTs were fabricated with an AlGaN/GaN-on-Si wafer (DOWA, Inc.) grown by metal-organic chemical vapor deposition (MOCVD). The cross-section is shown in Fig. 1. It consists of a 1.5 μm buffer structure followed by a 1.5 μm thick GaN layer grown on top of Si (111). Formation of the 2DEG was accomplished by growing an epitaxial stack consisting of a 1-nm-thick AlN spacer, 30-nm-thick $Al_{0.25}Ga_{0.75}N$ barrier layer and 1 nm thick GaN capping layer. This wafer has a manufacturer specified 2DEG mobility of ~1,400 cm^2/V-s and sheet density of ~$1x10^{13}$ cm^{-2} at room temperature. A mesa etch is used to define the

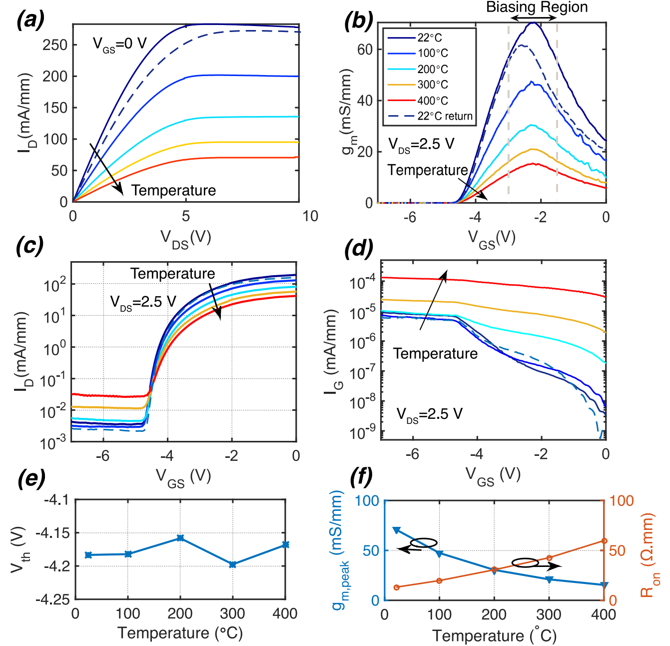

FIGURE 2. (a) The output characteristics (at $V_{GS} = 0$ V), (b) the transconductance (g_m) at $V_{DS} = 2.5$ V, (c) the $I_D - V_{GS}$ (at $V_{DS} = 2.5$ V) (d) the gate leakage current of the GaN HEMT over temperature from 22°C to 400°C, (e) temperature dependence of V_{th}, and (f) temperature dependence of $g_{m,peak}$ and R_{ON}.

HEMT channel via inductive coupled plasma with BCl_3/Cl_2 gases. Source/drain contacts were realized using a standard evaporation and lift-off process with a Ti/Al/Pt/Au (20/100/40/80 nm) stack. To make the contacts Ohmic, rapid thermal annealing (RTA) was employed at 850°C for 35 s. A layer of Pd/Au (40/10 nm) was e-beam evaporated and patterned as the gate metal. The devices were passivated by a 20 nm thick atomic layer deposited (ALD) Al_2O_3 layer, deposited at 250°C [32]. The contact pads were opened up by etching the ALD Al_2O_3 using a 20:1 buffered oxide etch (BOE) solution for 1 min. Ti/Pt (10/100 nm) is used for the interconnect/bond pads (Fig. 1). Before measurement, the devices were annealed at 600°C for 30 seconds in air on a hot-chuck.

III. EXPERIMENTAL RESULTS AND DISCUSSIONS

The GaN HEMTs were characterized in air from 22°C up to 500°C on a temperature-controlled probe station using an Agilent B1500A semiconductor parameter analyzer. The measurement at 22°C was repeated after cooling and denoted as 22°C return in Fig. 2.

A. DC CHARACTERISTICS OF THE ALGAN/GAN HEMT

The output characteristics ($I_D - V_{DS}$) and transconductance (g_m) of the HEMTs in the temperature range of 22°C to 400°C are shown in Fig. 2(a) and (b), respectively. The decrease in drain current (I_D) and g_m is due to lowered mobility at high temperatures. This decrease was observed to have a $T^{-1.5}$ dependence on temperature, consistent with the decrease in 2DEG electron mobility from optical phonon

scattering [33]. The peak of the transconductance ($g_{m,peak}$) remained constant over the entire temperature range from 22°C to 400°C at −2.3 V, and decreased to −2.5 V upon return to 22°C. This peak position defines an optimal biasing region for analog design, and its constancy over temperature is promising for future designs of ICs. The proposed biasing region for a temperature-stable analog amplifier design is indicated in Fig. 2(b).

It should be noted that the HEMT characteristics are partly recovered after cooling to room temperature, however, some degradation of both I_D and $g_{m,peak}$ could be observed. This can be attributed to the development of cracks at the AlGaN/GaN interface originated from the reduced piezoelectric polarization or strain relaxation [34].

Fig. 2(c) illustrates $I_D - V_{GS}$, showing the decrease of the HEMT *ON/OFF* ratio from $\sim 5\times10^4$ at room temperature to $\sim 10^3$ at 400°C. Moreover, the gate leakage current (I_G) of the HEMT over the temperature is observed to increase monotonically over temperature (from 10^{-5} to 10^{-4}), but recovered as the sample is cooled down to 22°C (Fig. 2(d)). The (V_{th}) of the HEMTs have been extracted using the *Extrapolation in the Linear Region* (ELR) method [35], considering the long-channel MOSFET model.

The variation of V_{th} over temperature is shown to be $\sim$ 0.9% (Fig. 2(e)), within the duration of the measurement (2-3 hours). Variation of $g_{m,peak}$ and the *ON* resistance (R_{ON}) over temperature is illustrated in Fig. 2(f), confirming the role of mobility decrease as previously discussed. Demonstration of high-temperature ICs in bipolar SiC technology [36], with similar performance degradation, suggests that with a good modeling endeavor, the relatively large variation of both $g_{m,peak}$ and R_{ON} could be considered in the design of ICs that could operate over the wide temperature range.

B. PROLONGED MEASUREMENTS AT 400°C AND 500°C (25 HOURS)

Electrical characterization of AlGaN/GaN HEMTs over prolonged exposure to high temperature was performed. Devices were placed on a hot-chuck in air for 25 hours, at 400°C and then 500°C. The DC characteristics of the HEMTs were recorded in 5-minute intervals. The devices measured in this experiment had previously been tested intermittently at elevated temperatures up to 500°C. Fig. 3(a)-(c) depict the output characteristics, the $I_D - V_{GS}$, and the V_{th} of the HEMTs at 400°C over the course of 25 hours. In all the aforementioned plots, little degradation is observed over time. The $I_D - V_{GS}$ characteristics stabilized after the 5 hours of operation at 400°C, as can be seen in Fig. 3(b). No variation of V_{th} from hour 5 to hour 25 was observed (Fig. 3(c)). However, when the temperature was increased to 500°C, measurements shows obvious degradation of the DC characteristics over time (Fig. 3(d)-(f)).

In these devices, n_{sh} is given by [37],

$$n_{sh} = \frac{\sigma_{tot}}{q} - \frac{\epsilon_0 \cdot \epsilon_{AlGaN}}{q^2 \cdot d}(q\phi_b + E_f - \Delta E_C), \quad (1)$$

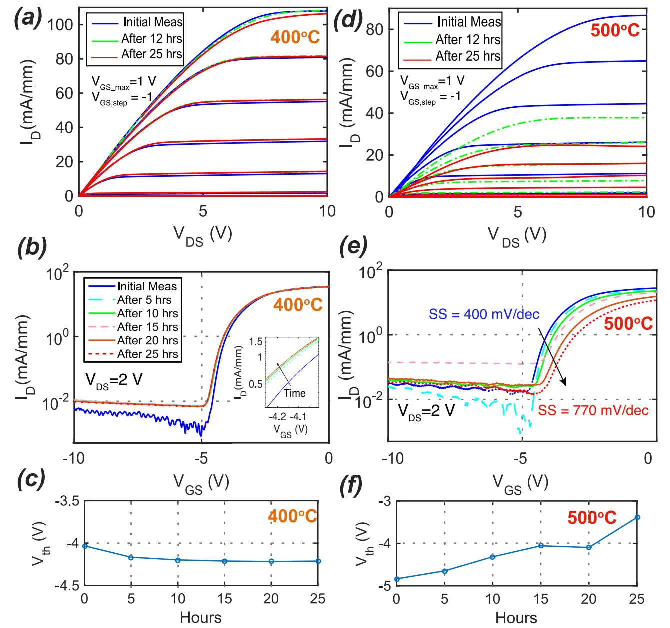

FIGURE 3. (a), (d) the output characteristics, (b), (e) $I_D - V_{GS}$ (at V_{DS} = 2 V), and (c) ,(f) the threshold voltage of the GaN HEMT (at V_{DS} = 2 V), at 400°C and 500°C over the course of 25 hours of measurement (the legend for (b) and (e) are the same).

where σ_{tot} is the total polarization charge (including both spontaneous and piezoelectric components), ϕ_b the Schottky barrier height, E_f the Fermi level with respect to the GaN conduction-band-edge energy at the AlGaN/GaN interface, ΔE_C the conduction band discontinuity at the AlGaN/GaN interface, q the elementary charge, d the thickness of the AlGaN barrier layer, ϵ_0 the permittivity of air, and ϵ_{AlGaN} the permittivity of AlGaN.

The degradation of the HEMT performance at 500°C over time is partly related to the reduction in the sheet density of the 2DEG (n_{sh}). It occurs due to *strain relaxation*, where a reduction in strain in the AlGaN barrier layer results in reduced piezoelectric polarization [34], [38]. The gate leakage current (I_G) at 500°C shows little variation ($\sim 5\times10^{-6}$) over 25 hours. This indicates that ϕ_b can be assumed to be constant over time. The variation of E_f and ΔE_C over time is also assumed negligible compared to the variation of σ_{tot}. In contrast to the measurements at 400°C, a monotonous reduction of $|V_{th}|$ is observed over time at 500°C as shown in Fig. 3(e),(f). The $|V_{th}|$ in a depletion-mode HEMT is given by [37],

$$|V_{th}| = \frac{q \cdot n_{sh} \cdot d}{\epsilon_0 \cdot \epsilon_{AlGaN}} \quad (2)$$

where only n_{sh} has a strong temperature dependency. The drastic reduction of $|V_{th}|$ at 500°C over time thus supports the role of *strain relaxation* in device degradation. If we assume that the drain current in the linear region follows a long-channel model, where $I_D \propto \mu[(V_{GS} - V_{th})(V_{DS}) - V_{DS}^2]$, and the mobility ($\mu$) does not change, we can estimate a $\sim$1.6× degradation in I_D from V_{th} degradation over the

25-hour duration. However, ~2.3× reduction of *ON*-state I_D is observed $V_{GS} = 0$ V (Fig. 3(e)) which indicates the 2DEG mobility decreased by a factor of ~1.4× over time at 500°C, besides the decrease in the 2DEG sheet density. The mobility degradation may also be associated with cracks developed at the AlGaN/GaN interface due to strain relaxation [34]. Moreover, the subthreshold slope shows a degradation over time from 400 mV/decade to 770 mV/decade (Fig. 3(e)), which is presumed to be associated with the interface traps, similar to Si MOSFETs [39], and is consistent with the similar study in AlGaN/GaN HEMTs [40]. Finally, the reported 25-hour operation is conducted as the preliminary study for understanding the effect of prolonged exposure of the HEMTs to high temperatures. Future efforts on reliability will be extended to stressed thermal cycling tests and longer exposure to high temperatures until device ultimate failure. Moreover, the choice of the substrate (Silicon, SiC or sapphire), passivation, buffer layer, and quality of the film growth are significant factors in the future development of AlGaN/GaN HEMTs for prolonged operation at elevated temperatures beyond 400°C.

IV. CONCLUSION

High-temperature operation of AlGaN/GaN HEMTs was demonstrated in the range of 22°C to 400°C in air. DC characterization of the HEMTs on a hot-chuck has been conducted showing V_{th} with less than 1% variation and $g_{m,peak}$ with negligible shift across V_{GS}, over the entire temperature range. Moreover, 25-hour measurements of the HEMTs show stable DC characteristics at 400°C, with a very slight degradation of I_D, and unchanged V_{th} after the initial burn-in. The HEMTs at 500°C exhibit a degradation behaviour over 25 hours which is attributed to the reduction of the 2DEG sheet density as well as mobility due to strain relaxation.

ACKNOWLEDGMENT

The advice from Prof. Jim Plummer is greatly acknowledged.

REFERENCES

[1] P. G. Neudeck, R. S. Okojie, and L.-Y. Chen, "High-temperature electronics—A role for wide bandgap semiconductors?" *Proc. IEEE*, vol. 90, no. 6, pp. 1065–1076, Jun. 2002.

[2] J. Y. Tsao *et al.*, "Ultrawide-bandgap semiconductors: Research opportunities and challenges," *Adv. Electron. Mater.*, vol. 4, no. 1, 2018, Art. no. 1600501.

[3] D. J. Spry, P. G. Neudeck, L. Chen, D. Lukco, C. W. Chang, and G. M. Beheim, "Prolonged 500°C demonstration of 4H-SiC JFET ICs with two-level interconnect," *IEEE Electron Device Lett.*, vol. 37, no. 5, pp. 625–628, May 2016.

[4] P. G. Neudeck *et al.*, "Yearlong 500°C operational demonstration of UP-scaled 4H-SiC JFET integrated circuits," in *Proc. Additional Conf. (Device Packag. HiTEC HiTEN CICMT)*, 2018, pp. 71–78. [Online]. Available: https://doi.org/10.4071/2380-4491-2018-HiTEN-000071

[5] J. A. Valle-Mayorga, A. Rahman, and H. A. Mantooth, "A SiC NMOS linear voltage regulator for high-temperature applications," *IEEE Trans. Power Electron.*, vol. 29, no. 5, pp. 2321–2328, May 2014.

[6] R. Murphree, S. Ahmed, M. Barlow, A. Rahman, H. Mantooth, and A. M. Francis, "A CMOS SiC linear voltage regulator for high temperature applications," in *Proc. Additional Conf. (Device Packag. HiTEC HiTEN CICMT)*, 2016, pp. 106–111. doi: 10.4071/2016-HITEC-106.

[7] M. Barlow, S. Ahmed, H. A. Mantooth, and A. M. Francis, "An integrated SiC CMOS gate driver," in *Proc. IEEE Appl. Power Electron. Conf. Expo. (APEC)*, Mar. 2016, pp. 1646–1649.

[8] R. R. Lamichhane *et al.*, "A wide bandgap silicon carbide (SiC) gate driver for high-temperature and high-voltage applications," in *Proc. IEEE 26th Int. Symp. Power Semicond. Devices IC's (ISPSD)*, Jun. 2014, pp. 414–417.

[9] L. Lanni, B. Malm, M. Östling, and C.-M. Zetterling, "500 °C bipolar integrated OR/NOR gate in 4H-SiC," *IEEE Electron Device Lett.*, vol. 34, no. 9, pp. 1091–1093, Sep. 2013.

[10] S. Kargarrazi, L. Lanni, and C.-M. Zetterling, "Design and characterization of 500 °C Schmitt trigger in 4H-SiC," in *Proc. Mater. Sci. Forum*, vol. 821, 2015, pp. 897–901.

[11] S. Kargarrazi, L. Lanni, S. Saggini, A. Rusu, and C.-M. Zetterling, "500 °C bipolar SiC linear voltage regulator," *IEEE Trans. Electron Devices*, vol. 62, no. 6, pp. 1953–1957, Jun. 2015.

[12] S. Kargarrazi, H. Elahipanah, S. Rodriguez, and C.-M. Zetterling, "500 °C, high current linear voltage regulator in 4H-SiC BJT technology," *IEEE Electron Device Lett.*, vol. 39, no. 4, pp. 548–551, Apr. 2018.

[13] S. Kargarrazi, L. Lanni, A. Rusu, and C.-M. Zetterling, "A monolithic SiC drive circuit for SiC Power BJTs," in *Proc. IEEE 27th Int. Symp. Power Semicond. Devices ICs (ISPSD)*, May 2015, pp. 285–288.

[14] S. Kargarrazi, L. Lanni, and C.-M. Zetterling, "A study on positive-feedback configuration of a bipolar SiC high temperature operational amplifier," *Solid-State Electron.*, vol. 116, pp. 33–37, Feb. 2016. [Online]. Available: http://www.sciencedirect.com/science/article/pii/S0038110115003470

[15] H. Elahipanah, S. Kargarrazi, A. Salemi, M. Östling, and C.-M. Zetterling, "500 °C high current 4H-SiC lateral BJTs for high-temperature integrated circuits," *IEEE Electron Device Lett.*, vol. 38, no. 10, pp. 1429–1432, Oct. 2017.

[16] M. Shakir, S. Hou, B. G. Malm, M. Östling, and C.-M. Zetterling, "A 600 °C TTL-based 11-stage ring oscillator in bipolar silicon carbide technology," *IEEE Electron Device Lett.*, vol. 39, no. 10, pp. 1540–1543, Oct. 2018.

[17] M. W. Hussain *et al.*, "A 500 °C active down-conversion mixer in silicon carbide bipolar technology," *IEEE Electron Device Lett.*, vol. 39, no. 6, pp. 855–858, Jun. 2018.

[18] S. Kargarrazi, H. Elahipanah, S. Saggini, D. Senesky, and C.-M. Zetterling, "500 °C SIC PWM integrated circuit," *IEEE Trans. Power Electron.*, vol. 34, no. 3, pp. 1997–2001, Mar. 2019.

[19] K. J. Chen *et al.*, "GaN-on-Si power technology: Devices and applications," *IEEE Trans. Electron Devices*, vol. 64, no. 3, pp. 779–795, Mar. 2017.

[20] G. Tang *et al.*, "Digital integrated circuits on an E-mode GAN power HEMT platform," *IEEE Electron Device Lett.*, vol. 38, no. 9, pp. 1282–1285, Sep. 2017.

[21] A. M. H. Kwan, X. Liu, and K. J. Chen, "Integrated gate-protected HEMTs and mixed-signal functional blocks for GAN smart power ICS," in *Proc. Int. Electron Devices Meeting*, Dec. 2012, pp. 7.3.1–7.3.4.

[22] M. Zhu and E. Matioli, "Monolithic integration of GaN-based NMOS digital logic gate circuits with E-mode power GaN MOSHEMTs," in *Proc. Int. Symp. Power Semicond. Devices ICs*, May 2018, pp. 236–239.

[23] P. Herfurth *et al.*, "GaN-on-insulator technology for high-temperature electronics beyond 400 °C," *Semicond. Sci. Technol.*, vol. 28, no. 7, Jul. 2013, Art. no. 074026. [Online]. Available: http://stacks.iop.org/0268-1242/28/i=7/a=074026?key=crossref.f27d87398160c762a1834a20921adb24

[24] D. Maier *et al.*, "Testing the temperature limits of GaN-based HEMT devices," *IEEE Trans. Device Mater. Rel.*, vol. 10, no. 4, pp. 427–436, Dec. 2010.

[25] D. Maier *et al.*, "InAlN/GaN HEMTs for operation in the 1000 °C regime: A first experiment," *IEEE Electron Device Lett.*, vol. 33, no. 7, pp. 985–987, Jul. 2012.

[26] F. Husna, M. Lachab, M. Sultana, V. Adivarahan, Q. Fareed, and A. Khan, "High-temperature performance of AlGaN/GaN MOSHEMT with SiO_2 gate insulator fabricated on Si (111) substrate," *IEEE Trans. Electron Devices*, vol. 59, no. 9, pp. 2424–2429, Sep. 2012.

[27] N. Maeda, K. Tsubaki, T. Saitoh, and N. Kobayashi, "High-temperature electron transport properties in AlGaN/GaN heterostructures," *Appl. Phys. Lett.*, vol. 79, no. 11, pp. 1634–1636, 2001. [Online]. Available: https://doi.org/10.1063/1.1400779

[28] D. Donoval, M. Florovič, D. Gregušovč, J. Kováč, and P. Kordoš, "High-temperature performance of AlGaN/GaN HFETs and MOSHFETs," *Microelectron. Rel.*, vol. 48, no. 10, pp. 1669–1672, 2008. [Online]. Available: http://www.sciencedirect.com/science/article/pii/S0026271408001200

[29] S. D. Burnham *et al.*, "Reliability characteristics and mechanisms of HRL's T3 GaN technology," *IEEE Trans. Semicond. Manuf.*, vol. 30, no. 4, pp. 480–485, Nov. 2017.

[30] A. J. Suria, A. S. Yalamarthy, H. So, and D. G. Senesky, "DC characteristics of ALD-grown Al_2O_3 /AlGaN/GaN MIS-HEMTs and HEMTs at 600 °C in air," *Semicond. Sci. Technol.*, vol. 31, no. 11, 2016, Art. no. 115017. [Online]. Available: http://stacks.iop.org/0268-1242/31/i=11/a=115017

[31] G. Via *et al.*, "Gate optimization of AlGaN/GaN HEMTs using WSi, Ir, Pd, and Ni Schottky contacts," in *25th Annu. Tech. Dig. IEEE Gallium Arsenide Integr. Circuit (GaAs IC) Symp.*, 2003, pp. 277–279.

[32] T. Hashizume, S. Ootomo, and H. Hasegawa, "Suppression of current collapse in insulated gate AlGaN/GaN heterostructure field-effect transistors using ultrathin Al_2O_3 dielectric," *Appl. Phys. Lett.*, vol. 83, no. 14, pp. 2952–2954, 2003. [Online]. Available: https://doi.org/10.1063/1.1616648

[33] W. S. Tan, M. J. Uren, P. W. Fry, P. A. Houston, R. S. Balmer, and T. Martin, "High temperature performance of AlGaN/GaN HEMTs on Si substrates," *Solid-State Electron.*, vol. 50, no. 3, pp. 511–513, 2006.

[34] M. Hou *et al.*, "Degradation of 2DEG transport properties in GaN-capped AlGaN/GaN heterostructures at 600°C in oxidizing and inert environments," *J. Appl. Phys.*, vol. 122, no. 19, Nov. 2017, Art. no. 195102. [Online]. Available: http://aip.scitation.org/doi/10.1063/1.5011178

[35] A. Ortiz-Conde *et al.*, "A review of recent MOSFET threshold voltage extraction methods," *Microelectron. Rel.*, vol. 42, nos. 4–5, pp. 583–596, 2002.

[36] C.-M. Zetterling *et al.*, "Bipolar integrated circuits in SiC for extreme environment operation," *Semicond. Sci. Technol.*, vol. 32, no. 3, 2017, Art. no. 034002.

[37] A. S. Yalamarthy and D. G. Senesky, "Strain- and temperature-induced effects in AlGaN/GaN high electron mobility transistors," *Semicond. Sci. Technol.*, vol. 31, no. 3, Mar. 2016, Art. no. 035024. [Online]. Available: http://stacks.iop.org/0268-1242/31/i=3/a=035024?key=crossref.7d13cb84a67d49cffebb42c8956c1078

[38] D. J. Chen *et al.*, "Temperature-dependent strain relaxation of the AlGaN barrier in AlGaN-GaN heterostructures with and without Si_3N_4 surface passivation," *Appl. Phys. Lett.*, vol. 88, no. 10, Mar. 2006, Art. no. 102106. [Online]. Available: http://aip.scitation.org/doi/10.1063/1.2186369

[39] S. Sze, *Physics of Semiconductor Devices*. New York, NY, USA: Wiley-Intersci., 1981. [Online]. Available: https://books.google.com/books?id=LCNTAAAAMAAJ

[40] J. W. Chung, X. Zhao, and T. Palacios, "Estimation of trap density in AlGaN/GaN HEMTs from subthreshold slope study," in *Proc. 65th Annu. Device Res. Conf.*, Jun. 2007, pp. 111–112.